Fermilab

TM-1286
1610.000
Dec. 14, 1984

MAGNETIZATION MEASUREMENTS OF SOME SUPERCONDUCTING CABLES

M. Kuchnir

Fermi National Accelerator Laboratory
Batavia, Illinois 60510

and

A.K. Ghosh

Brookhaven National Laboratory
Upton, New York 11973

ABSTRACT

We report here, magnetization measurements on 5 samples of Fermilab Superconducting Cable. These measurements are needed to provide a quantitative basis for the understanding of the current dependent sextupole and decapole fields in superconducting dipole magnets due to persistent currents. This understanding is relevant both to the design of the SSC large dynamic range magnets[1] and to the interpretation of the persistent current fields in Energy Saver magnets[2]. These measurements were carried out at Brookhaven National Laboratory on October 1 and 2, 1984 with the same equipment and procedures of the measurements described by A.K. Ghosh, K.E. Robins and W.B. Sampson[3].

INTRODUCTION

The strands of a Fermilab-Rutherford cable are formed from a multifilamentary superconductor wire. This wire is made up of a bundle of twisted NbTi filaments embedded in a copper matrix. Persistent currents flowing through the filaments cause residual magnetic fields with hysteretical characteristics. These wires can be treated as made out of a material with anisotropic electrical and magnetic properties. When superconducting, their electrical resistance is zero longitudinally but not transversally, because of the copper matrix. This resistance is the cause of the few nΩ observed in a 3" cable splice. Their magnetization is the subject of this memo. We do not consider here the time dependent effect of internal electric currents between filaments which is essentially cancelled by the twist in the wire.

MEASUREMENTS

Whether the origin of the magnetization is atomic-molecular or due to superconducting persistent currents the magnetization can be measured by its effect in the magnetic field distribution. This can be accomplished, for instance, by measuring the change in the inductance of a solenoid due to the introduction of the sample in its uniform field region. The shape of the sample can be selected to be elipsoidal in order to simplify the demagnetization factor. This factor corrects for the difference between the local field inside the sample and the field just outside the sample.

Since the purpose of this measurement is to quantify the magnetization of superconducting cables, the samples used consisted of 3 pieces cut from the same cable, each 12"±.03" long, stacked with the wider face perpendicular to the external magnetic field, H. These samples are labeled as 0274, 2120, 2602, 2629 and 4008 after the Reel Number of their origin. Table I presents the fabrication as well as other characteristics of these cables. Some of which were obtained from observation of their cross section under microscope.

Table I - Sample Characteristics

Reel No.	0274	2120	2602	2629	4008
fil. diam.	8.7 μm	8.7 μm	19.3 μm	8.7 μm	8.7 μm
no. strands	23*	23	23	23	23
crop'd strands	2	4	0	0	0
Cu:sc ratio	1.8:1	1.8:1	1.37:1	1.8:1	1.8:1
wire diam.	.0268"	.0268"	.0268"	.0268"	.0268"
fil./strand	2070	2070	510	2070	2070
wire twist/in.	2	2	2	2	2
strand coat	staybrite	ebonol	staybrite	zebra	staybrite
insulation	none	none	kapt+Bstg	kapt+Bstg	none
I_c (5 T)	5320 A 5260 A	4830 A 5330 A	6650 A	6230 A	4750 A 5500 A
I_c (7 T)	--	--	4215 A	--	--
comment	--	--	ES low β	RA1001	RA1001 bus

* of these 14 strands have no copper core

More specifically, the measurements consisted in:
1) installing the sample in the middle of one of a pair of balanced pick-up-coils in liquid helium (see figure 1).

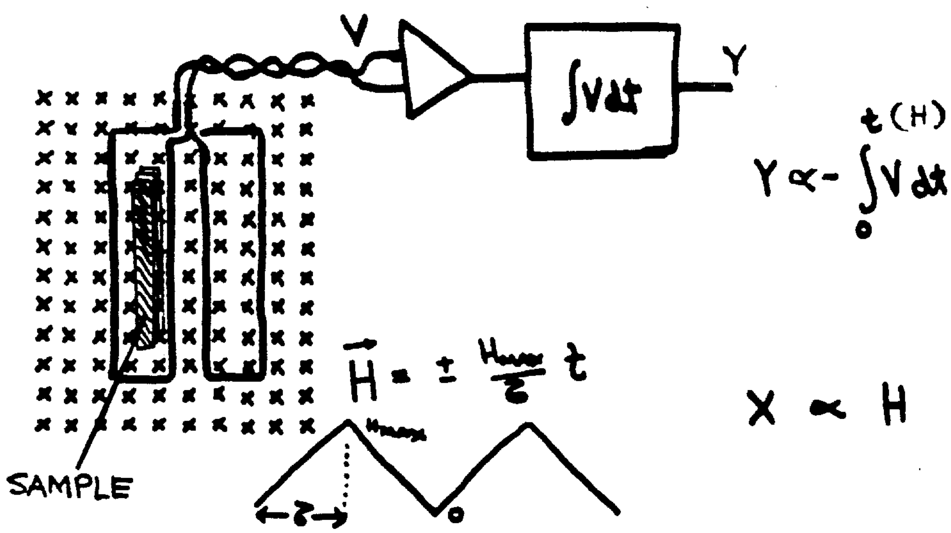

Figure 1. Magnetization measurement concept

These pick-up-coils are used instead of a solenoid in order to maximise the signal. A sample of known magnetization is used for calibration eliminating the need to compare these pick-up-coils with the solenoid.

2) activating the external uniform magnetic field. This field, perpendicular to the wide face of the cables in the sample, is set to follow a triangular wave,

$$H = \pm(H_{max}/\tau)\ t$$

ramping linearly with time from 0 at $t=0$ to H_{max} at $t=\tau$, to 0 at $t=2\tau$ etc.

3) recording this field, or the current that generates it, as a function of time. This is one of the main parameters.

4) recording the integral with respect to time of the e.m.f. at the pick-up-coil terminals. This integral is proportional to the flux of the magnetic field H . S :

$$-V = \frac{d}{dt}(H\ .\ S)$$

or in terms of the magnetic induction, B, and the magnetization M

$$-\frac{1}{S} V = \frac{d}{dt}(\ B - \mu_o\ M\ )$$

$$-\frac{1}{S}\int V\ dt = (\ B_{max}/\tau\ )\ t - \mu_o\ M$$

5) repeating the above procedure without the sample

$$-\frac{1}{S}\int V_o\ dt = (\ B_{max}/\tau\ )\ t$$

and subtracting its result from the procedure with the sample.

$$\mu_o\ M = \frac{1}{S}\int V_o\ dt - \frac{1}{S}\int V\ dt$$

The magnetization M is a function of H history. The upper limit of the integrals is the time at which the field is H. The integration is done by the low drift integrator described by C.R. Walters and M.G. Thomas[4]. Both H, as a voltage proportional to the current through the 5 T dipole magnet CM-1 that generates it, and μ_o M as the output of the integrator are recorded in quadrants of the memory of a Nicolet 2090 digital osciloscope. The calibration constants in the present measurements were 0.69 mT/(mV.s) and 1.15 mT/mV. In order to have reproducible results for M(H) the sample is subjected to one full cycle of H (i.e. 0 to H_{max} to 0) before recording the data. The half period τ was of the order of several minutes. The data was monitored by an X Y recorder during its acquisition, a procedure that permited observation of drift effects, paramagnetic or diamagnetic components. Several cycles of period 2τ are therefore involved in the data acquisition. The last one with the sample in is cut short (fast drop in H) to check for eddye current effects. These cables did not present any in these measurements. After the acquisition, the four quadrants of the Nicolet memory containing the with sample and without sample data, are copied into a diskette and transfered to an HP9836 computer for processing, systematic corrections, examination and plotting. More information on calibration and systematic errors compensation are presented in the discussion and in reference (3).

The results are shown in figures 2 trough 6. In these plots, please observe that the scales are not the same. The horizontal axis presents $\mu_o H$ in Teslas and the vertical axis is $\mu_o M$ in milliTeslas (mT) or 1.038 mT (correction factor introduced after the plot). The samples are identified by Reel No. and BNL Nicolet data diskette No. (i.e. 28-1, etc).

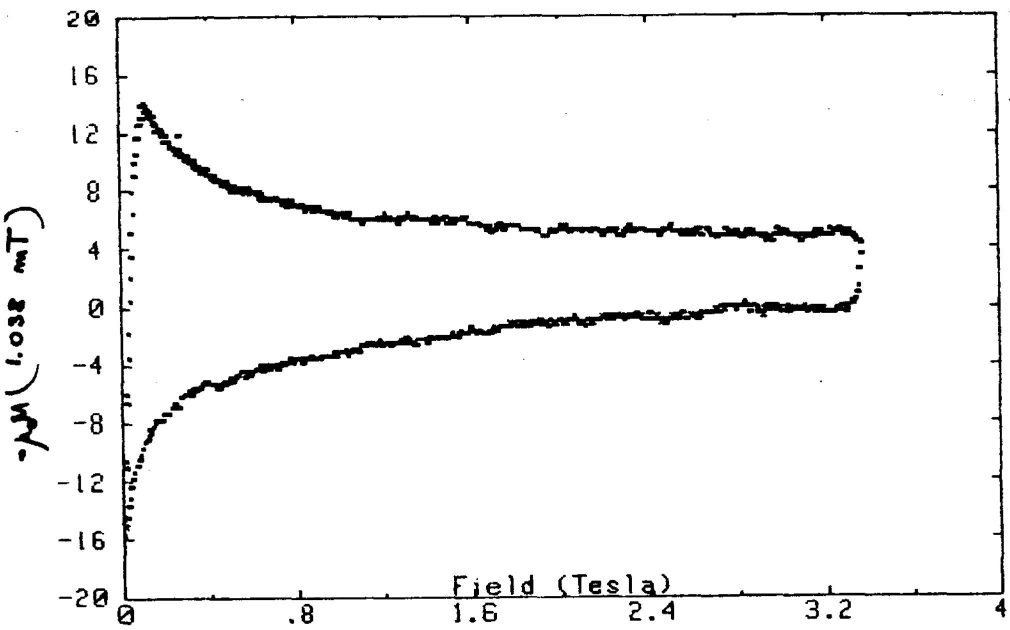

Figure 2. Magnetization Data for Sample 0274

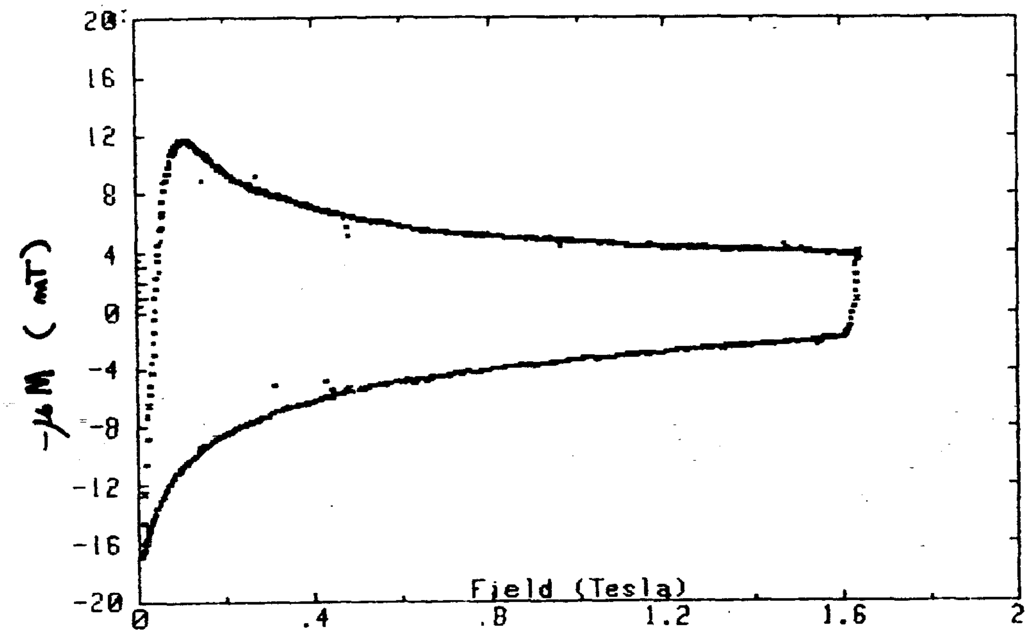

Figure 3. Magnetization Data for Sample 2120

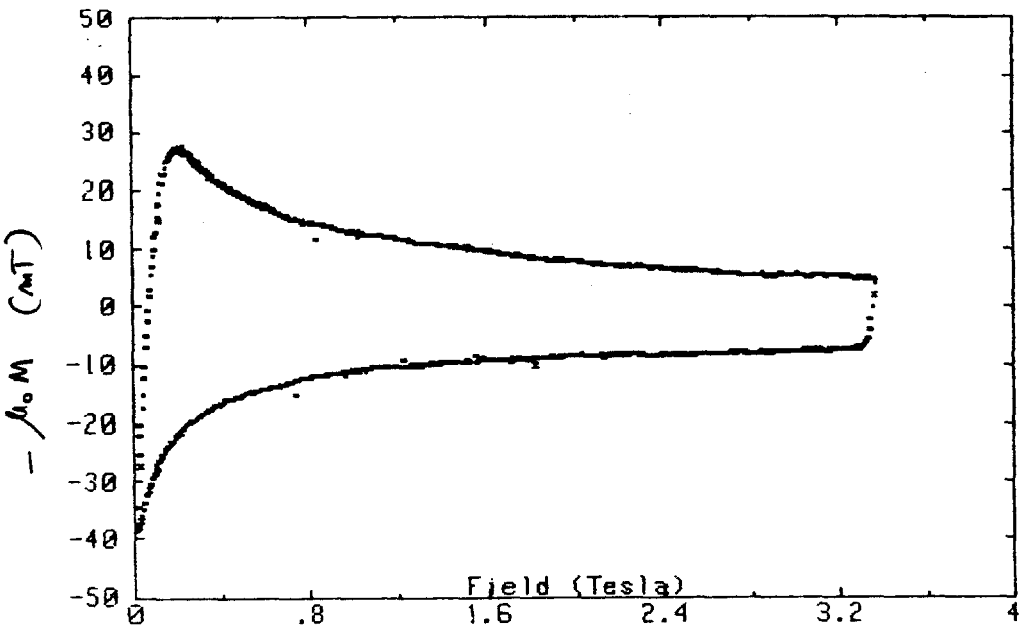

Figure 4. Magnetization Data for Sample 2602

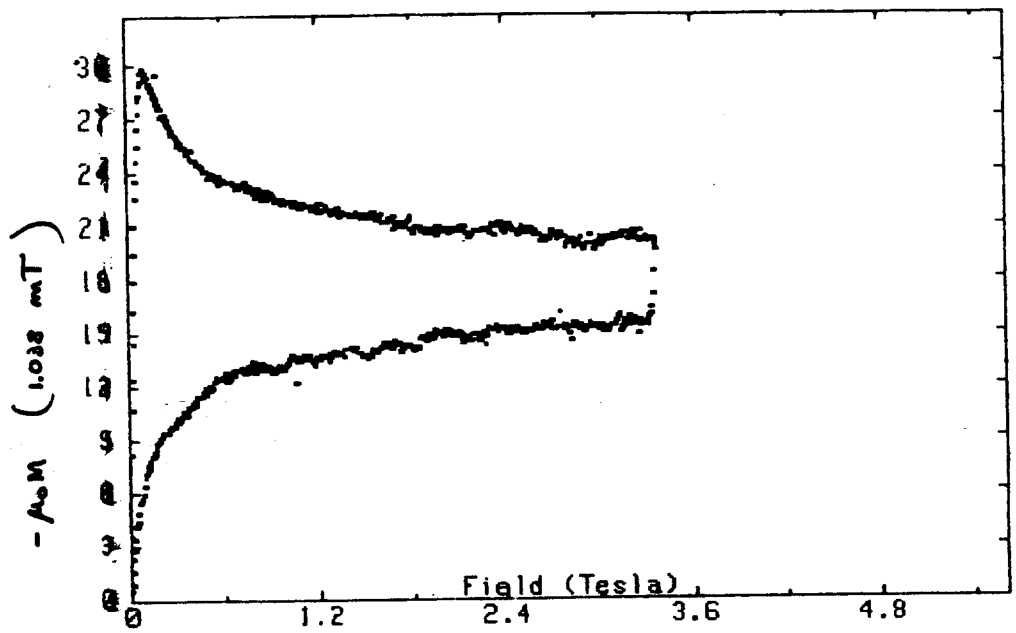

Figure 5. Magnetization Data for Sample 2629

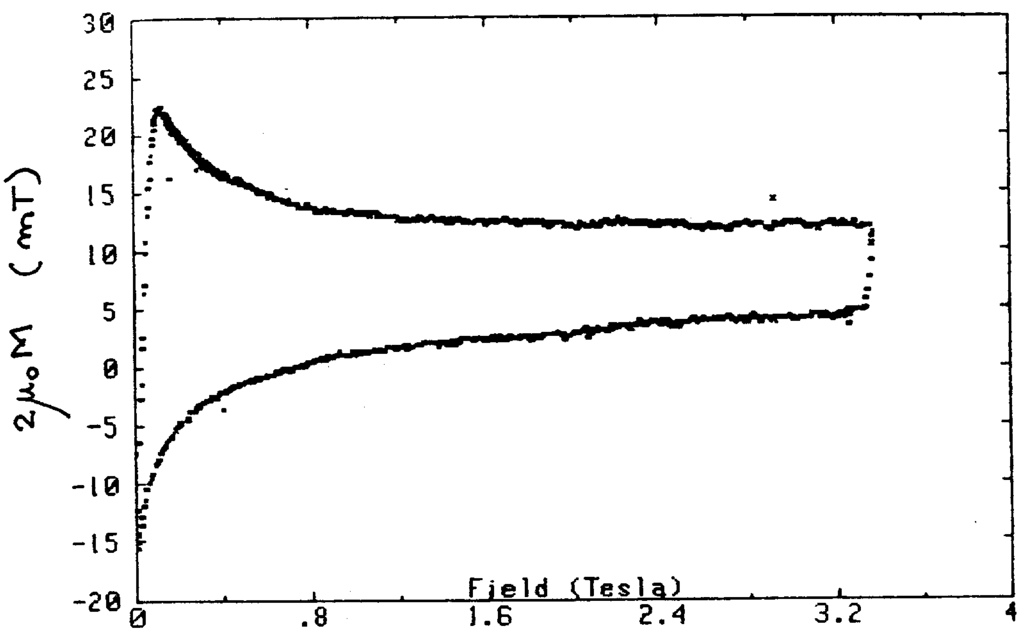

Figure 6. Magnetization Data for Sample 4008

DISCUSSION

The vertical width of the plots in figures 2 through 6 is the difference between the magnetization when H is increasing and the magnetization when H is decreasing. Figure 7 presents this difference in magnetization as calculated from the data. This is a function of the hysteretic cycle being used. In our case, which is the relevant case for SSC magnets, this variation is a triangular wave of just one polarity.

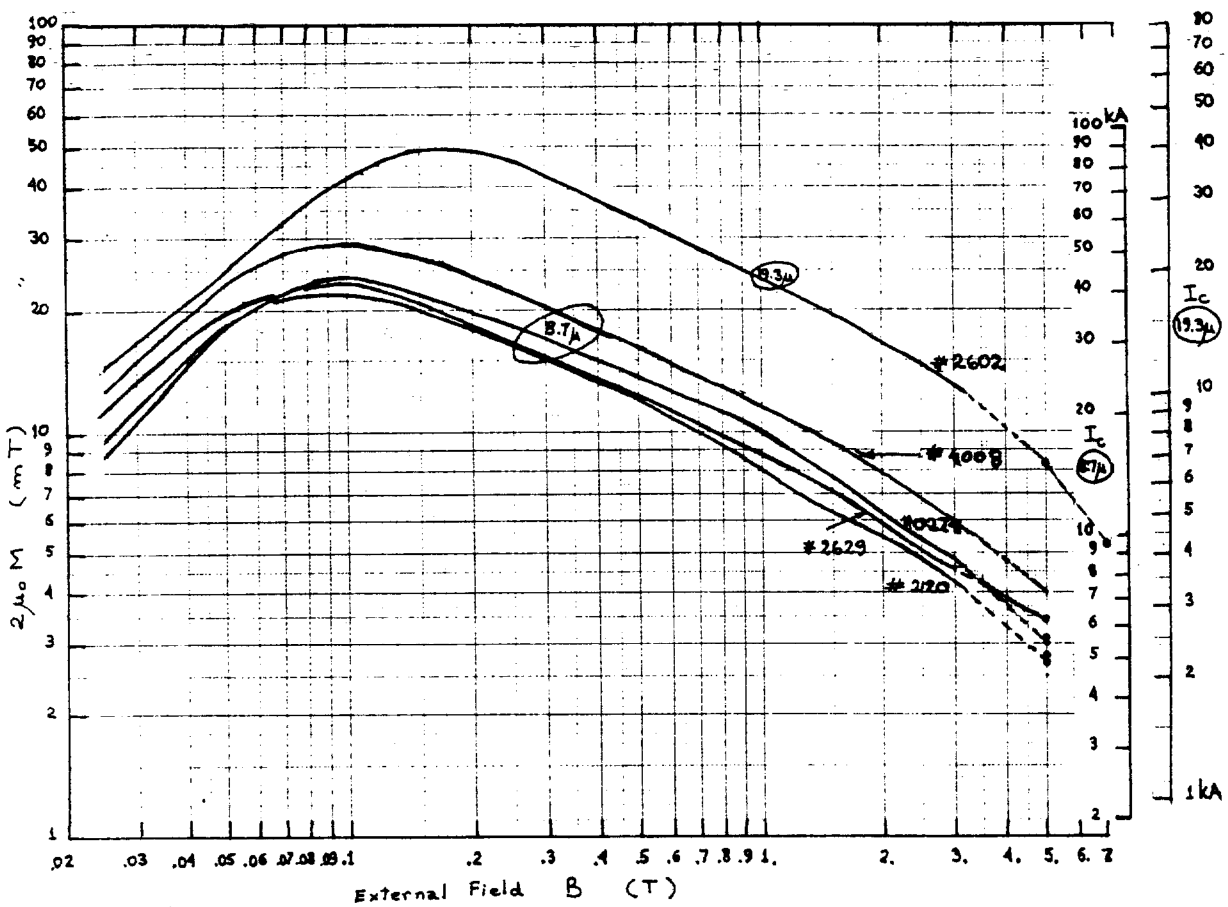

Figure 7. Difference in Up and Down Ramping Magnetization

The horizontal scale 3 mT resolution used in the measurement of the external field is less than the random noise. The vertical scale resolution depended on the field range used in the run (±.2 mT for 0-1.6 T range and ±.45 mT for 0-3.2 T range). Drifts in the integrator and error in synchronising the ramp trigger affect the vertical scale in a systematic way, which after correction presents a reproducibility usually better than ±1 mT.

THE CRITICAL-STATE CURRENT MODEL

There are models that permit us associate the difference in magnetization with the persistent current distribution in the wire. The so called critical-state model assumes that in a filament the current density is zero or either $+J_c/-J_c$ where J_c is the critical current density of the filament. This assumption comes from the idea of how the current in the filament reacts to the raising of the external field by an amount ΔB perpendicular to the filament. Starting from zero field, the first amount ΔB will initially induce a current to flow in the surface of the filament at a very high current density trying to prevent the field from penetrating it. Because this current density is higher than J_c the surface current will decay resistively and the magnetic field will start to penetrate the interior of the filament. As soon as the current density falls to J_c, however, decay will cease and the current density will remain constant. The result of this process will be that, in the steady state, the filament will be left with two oppositely-directed stripes of current flowing at critical density on opposite sides. The thickness of the stripes is not uniform, it can be obtained as follows: from

$$\mathrm{curl}\,\vec{B} = \mu_o \vec{J}$$

in a radial plane we get

$$\Delta B/p = \mu_o J_c$$

where p is the penetration depth of the field or the local stripe thickness. A second increment ΔB produces similar effects, with a penetration to a depth $2\Delta B/\mu_o J_c$. This process continues until the whole filament is carrying current at density J_c, at which point the field has fully penetrated. Further increases in field will now penetrate the whole filament; they do not cause any change in the screening-current pattern which simply flows at critical density in opposite directions in each half of the filament. A transport current along the filament will cause this pattern to become assymetric. A reversal of the external field will start modifying this pattern in the same way, from the edges towards the center.

The magnetization of the wire is equal to the magnetic moment of the current per unit volume, by definition. Each filament of radius, a, fully penetrated has a magnetic moment per unit length given by

$$\Gamma = \int_{-a}^{+a} J(x).x.2\sqrt{a^2-x^2}.dx$$

since $J(x)=J_c(H)$:

$$\Gamma = 4\ J_c(H)\ [\tfrac{1}{3}(a^2-x^2)^{\frac{3}{2}}]_o^a$$

$$\Gamma = \frac{4}{3}\ J_c(H)\ a^3$$

since the strand volume per unit length is A the magnetization per strand with N filaments is

$$M = N\ \Gamma/A = (4/3)\ N\ J_c\ a^3/A$$

For a multifilamentary wire (strand) of cross-section area, A, and fraction of superconductor $\lambda=N\pi a^2/A=(1+Cu/Sc)^{-1}$ the critical current, i_c, and the critical current density, J_c, can be expressed as

$$i_c = \lambda\ J_c\ A \quad \text{and} \quad J_c = (3\pi/4)\ M/\lambda a = (3x10^7/32).2\mu_o M/\lambda a$$

or the magnetization as

$$M = (4/3\pi)\ \lambda\ J_c\ a$$

stressing the linear dependence on the filament radius. For a cable with 23 strands the critical current, I_c, is

$$I_c = 23\ (3x10^7/32)\ (A/a)\ 2\mu_o M.$$

We can now interpret the features in figure 7. On the right side of the maximum, $2\mu_o M$ corresponds to twice the magnetization of a cable with fully penetrated filaments, while on the left side $2\mu_o M$ results from partial filament penetration or a $+J_c/-J_c$ pattern characteristic of the hysteretic cycle being carried out. The maximum itself occurs at the field where full penetration is obtained. For fields to the right of the maximum we can associate a cable with a given filament size to a critical current. For our samples in figure 7 this is done with the right side scales. This association is not valid for partially penetrated filaments. With different hysteretic cycles than the one we used it is possible to extend this association to lower fields and larger critical currents, but a correction has to be made accounting for the self-field of transport currents. The prediction of critical current from magnetization measurements assumes the filaments to be continuous. A wire can have broken filaments with consequent low critical current and this condition will not show up in its magnetisation.

AKNOWLEDGEMENTS

We thank W.B. Sampson and H.E. Fisk for support and F. Markley and D. Muniz for preparing the cross-sections of the cables for microscopic observation.

REFERENCES

1. B.C. Brown and H.E. Fisk, "A technique to minimize persistent current multipoles in superconducting accelerator magnets", Applied Sup. Conf., San Diego, Calif., Sep 9-13, (1984)

2. B.C. Brown, H.E. Fisk and R. Hanft, "Persistent current fields in Tevatron magnets", Applied Sup. Conf., San Diego, Calif., Sep 9-13, (1984)

3. A.K. Ghosh, K.E. Robins and W.B. Sampson, "Magnetization measurements on multifilamentary Nb_3Sn and NbTi conductors", Applied Sup. Conf., San Diego, Calif., Sep 9-13, (1984)

4. C.R. Walters and M.G. Thomas, "A Low Drift Integrator", Informal Report BNL-19071 AADD 74-4 (June 5, 1974)